# Resolving the EPR Spectra in the Cytochrome $bc_1$ Complex from *Saccharomyces cerevisiae*

**Fraser MacMillan · Christian Lange · Matt Bawn · Carola Hunte**

**Abstract** Quinone molecules are ubiquitous in living organisms. They are found either within the lipid phase of the biological membrane (quinone pool) or are bound in specific binding sites within membrane-bound protein complexes. The biological function of such bound quinones is determined by their ability to be reduced and/or oxidized in two successive one-electron steps. As a result, quinones are involved as one- or two-electron donors or acceptors in a large number of biological electron-transfer steps occurring during respiratory or photosynthetic processes. The intermediate formed by a one-electron reduction step is a semiquinone, which is paramagnetic and can be studied by electron paramagnetic resonance (EPR) spectroscopy. Detailed studies of such states can provide important structural information on these intermediates in such electron-transfer processes. In this study, we focus on the redox-active ubiquinone-6 of the yeast cytochrome $bc_1$ complex (QCR, ubiquinol: cytochrome $c$ oxidoreductase) from *Saccharomyces cerevisiae* at the so-called $Q_i$ site. Although the location of the $Q_i$ binding pocket is quite well known, details about its exact binding are less clear. Currently, three different X-ray crystallographic studies suggest three different binding geometries for $Q_i$. Recent studies in the bacterial system (*Rhodobacter sphaeroides*) have suggested a direct coordination to histidine as proposed in the chicken heart crystal structure model. Using the yeast system we apply EPR and especially relaxation filtered hyperfine

F. MacMillan (✉) · M. Bawn
Henry Wellcome Unit for Biological EPR, School of Chemical Sciences and Pharmacy,
University of East Anglia, Norwich NR4 7TJ, UK
e-mail: fraser.macmillan@uea.ac.uk

C. Lange
Department of Molecular Membrane Biology,
Max Planck Institute of Biophysics, 60438 Frankfurt, Germany

C. Hunte
Institute of Membrane and Systems Biology, University of Leeds, Leeds, UK

(REFINE) spectroscopy to study the $Q_i$ binding site. ^{14}N-electron spin-echo envelope modulation spectroscopy together with an inversion-recovery filter (REFINE) is applied to resolve the question of whether ^{14}N modulations arise from interactions to $Q_i^{\bullet-}$ or to the Rieske iron–sulphur center. These results are discussed with regard to the location and potential function of $Q_i$ in the enzyme.

## 1 Introduction

The cytochrome $bc_1$ complex (QCR, ubihydroquinone:cytochrome $c$ oxidoreductase, EC 1.10.2.2) is an energy-transducing membrane protein complex, which participates in respiration and photosynthesis (for recent reviews see, e.g., Refs. [1, 2]). The enzyme transfers electrons from ubihydroquinone to cytochrome $c$ and couples this process to the translocation of protons across the membrane. An essential feature of this mechanism, which is known as the proton motive Q cycle [3], is the localization of the two catalytic sites for ubiquinone redox reactions on opposite sides of the membrane (Fig. 1a). During the first half of the Q cycle one molecule of ubiquinol is oxidized at the $Q_o$ site in a bifurcated manner. One electron is transferred to the acceptor cytochrome $c$ via two catalytic subunits, namely the Rieske protein and cytochrome $c_1$. The second electron is transferred via the third catalytic subunit cytochrome $b$ (heme $b_L$ and heme $b_H$) to the $Q_i$ site, at which a bound ubiquinone molecule is reduced to ubisemiquinone. During the second half of the Q cycle a second ubiquinol molecule is oxidized at the $Q_o$ site, resulting in reduction of a second molecule cytochrome $c$, full reduction of the bound ubisemiquinone and subsequent ubiquinol release. Protons are taken up from the electronegative side for ubiquinone reduction and they are released towards the electropositive side upon ubiquinol oxidation. Exact mechanistic details of this mechanism still remain controversial.
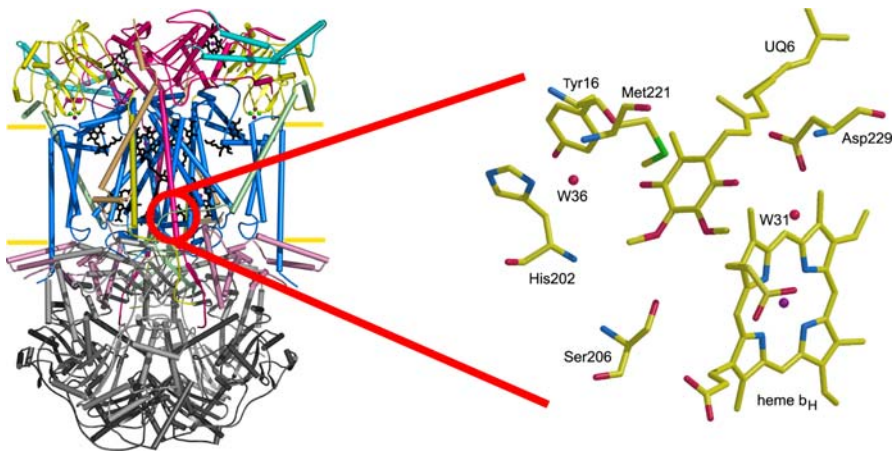


**Fig. 1** *Left* Structure of yeast cyt $bc_1$ complex (Protein Data Bank, 1kb9) with redox-active cyt $b$, cyt $c_1$ and Rieske protein in *blue*, *pink*, and *yellow*, respectively. *Right* Cofactor and ligands; ubiquinone-6 (UQ$_6$) at the $Q_i$ site

Ubiquinone binding sites, present in several respiratory and photosynthetic complexes, are fundamental elements of the different molecular mechanisms of these complexes. The binding sites control the chemical properties of the respective quinone, so that it can function more effectively in electron- and proton-transfer kinetics. Such a control mainly occurs through hydrogen bonds to the two carbonyl groups, but may also involve $\pi$-interactions with aromatic amino acids.

The $Q_i$ site of the cytochrome $bc_1$ complex has to stabilize binding of both ubiquinone as well as ubisemiquinone and has to permit proton transfer most likely via hydrogen bonds. Three X-ray structures of bovine and yeast complexes provide controversial information, as they show different substrate binding patterns. In the structure of the yeast cytochrome $bc_1$ complex [4, 5], the carbonyl oxygen atoms of the natural substrate coenzyme $Q_6$ ($UQ_6$) are in hydrogen-bonding distance to a water molecule as well as to aspartate Asp229 of cytochrome $b$ on one side, and to a water molecule that is stabilized by histidine His202 of cytochrome $b$ on the other side (Fig. 1b). It was suggested that a water molecule is the primary proton donor on one side and that the second proton is either donated by a water molecule or Asp229 [4–6]. In contrast, in the model of the bovine complex from Berry's group [7], serine Ser205, His201 and Asp228 of cytochrome $b$ are ligands of the quinone head group. Each of the two latter residues is in a position for direct hydrogen bonding with one of the quinone carbonyl oxygen atoms, suggesting a direct proton transfer. However, in contrast, Xia's [8] group described for the structure of the bovine complex that both the histidine and aspartate hydrogen bonds are mediated by water molecules.

Proton-transfer reactions are likely to be mediated via hydrogen bonds and it is clearly a matter of debate, whether water molecules may act as primary proton donors during ubiquinone reduction. The observed differences in the two bovine and the yeast structure may be species related and/or due to different redox states of the structures. The redox state of the $bc_1$ complexes in the different structures described above is not clear. The complexes are most likely only partially reduced, and it has to be expected that the substrate molecule is bound in its oxidized form.

With electron paramagnetic resonance (EPR) spectroscopic analysis the environment of the substrate can be analyzed for a defined redox state, namely for the semiquinone. While only very recently first observations [9, 10] of a trapped semiquinone intermediate have been reported at the $Q_o$ site, although their origin has been disputed [11], the radical state $Q_i^{\bullet-}$ has long been detectable using X-band continuous-wave (cw)-EPR spectroscopy [12]. X-band cw electron-nuclear double resonance (ENDOR) spectroscopy has been performed on $Q_i^{\bullet-}$ from the purified beef heart $bc_1$ complex, and exchangeable features assigned to hydrogen-bonded protons were detected by comparison of the spectra measured in $H_2O/D_2O$ medium, as well as hyperfine couplings with protons of the quinone ring itself [13]; however, the specific assignments remain unclear.

Electron spin-echo envelope modulation (ESEEM) spectroscopy is also a powerful method to study semiquinones in proteins [14]. It can provide information about the binding partners from the protein to the radical anion. Previously this method has been applied to study the stable electron acceptors of the bacterial reaction centres [15, 16], as well as photosystems I and II of higher plants [17–19]. Indeed the specific assignments made by some of these experiments predated the

resolution of the three-dimensional structures, which were later confirmed by such structural models. More recently, ESEEM data on the terminal quinol oxidase from *E. coli* has predicted a direct interaction with a nitrogen atom [20], which has very recently been further characterized [21], but as yet no bound quinones have been observed in the crystal structure model [22]. More recently similar experiments have been performed on the bacterial $bc_1$ complex from *Rhodobacter (Rb.) sphaeroides* and a direct binding to histidine has been proposed [23, 24].

When applying EPR spectroscopy to study electron-transfer intermediates in mitochondrial or bacterial respiratory chains, it is important to realize that presence of several paramagnetic species is a common occurrence. This can have important consequences, especially when using cw-EPR, as it may appear due to the use of field modulation that these different species, which contribute to the overall EPR spectrum, are not overlapping. Since the expansion of the application of modern pulsed EPR methods [14] to study such complex biological systems in much greater detail, the phenomenon of such overlapping spectra has to be considered more carefully.

One important prerequisite for the analysis and assignment of specific experimental observations in biological samples is the ability to study contributions, which arise from specific species, individually and directly. In principle, there are several ways in which such paramagnetic species can be distinguished; first, by biochemical means or through use of molecular biology. Although these methods are applied extensively, it may sometimes not be possible to remove certain contributions to the overall spectrum, while maintaining the correct redox state for the species to be investigated by EPR. In the case of molecular biology, the removal of an important amino acid residue or prosthetic group may and often does lead to lack of formation of the whole protein under consideration.

In principle, one can also distinguish these species spectroscopically. Let us consider their EPR parameters. There are several ways in which the EPR spectrum can be resolved; if the paramagnetic species under study have different $g$ values, then performing multi-frequency EPR experiments can spectrally separate them. High-field EPR spectroscopy [25] is now commonly used as higher magnetic fields lead to a higher spectral resolution of the EPR spectrum, especially for organic radicals. If the overlapping species have different electronic spin quantum numbers $S$ and $m_s$ (e.g., in the case of an organic radical and certain metal centres), they can be distinguished by their different Rabi oscillation (nutation) frequencies [26]. Using the temperature dependence, differences in spin–lattice relaxation times ($T_{1e}$) can also be exploited to distinguish between different species, and it may be possible to suppress the contribution of one species [27] in order to study a second species in greater detail.

Under the reducing conditions where one usually observes a stable semiquinone radical anion in the $Q_i$ site of the $bc_1$ complex, the Rieske iron–sulphur center is also reduced and paramagnetic. The EPR signal from the semiquinone overlaps with the much broader Rieske EPR signal. Thus, in order to study the interaction of $Q_i^{\bullet-}$ with the protein environment directly using ESEEM spectroscopy in the yeast QCR, it is important to resolve its EPR spectrum from that of the underlying Rieske iron–sulphur center.

Recently, a technique of relaxation filtered hyperfine (REFINE) spectroscopy was introduced, through which the characterization of the important FeS center N2 in complex I was performed [28]. It was not possible to study this FeS center individually in complex I using pulsed EPR, and this technique was thus successfully developed to address the question of the amino acid coordination of this center in the protein. In the experiment a pulse sequence was used which includes an inversion-recovery pulse applied together with a standard Hahn-echo detection sequence [29], which allows the separation of different paramagnetic species by differences in their longitudinal relaxation times ($T_{1e}$). The time between the inversion-recovery pulse and the detection sequence is varied, and depending on this so-called filter time ($T_F$), it is possible to selectively suppress one of the two overlapping EPR species and thus record the individual EPR spectrum of a second species [28, 30].

Here, we apply this technique to resolve the individual EPR spectra from the $Q_i^{\bullet-}$ and the Rieske FeS center in the $bc_1$ complex. The goal is to determine the conditions where it is possible to study these species individually within such mixtures in greater detail using hyperfine spectroscopy (ENDOR, ESEEM), in order to ultimately address the question of direct coordination of the $Q_i$ semiquinone to histidine or to water.

## 2 Experimental

### 2.1 Protein Purification and Characterization

The cytochrome $bc_1$ complex was purified from the yeast *Saccharomyces cerevisiae* following the published protocol [31, 32]. After addition of one equivalent coenzyme $Q_6$ (20 mM stock in dimethyl sulfoxide), the enzyme was concentrated using ultrafiltration (Centriprep 30, Amicon). Buffer exchange was accomplished using a small desalting column (PD-10, Pharmacia) equilibrated with 250 mM NaCl, 50 mM Tris/HCl (pH 8.0), 0.015% dodecyl maltoside. The pooled fractions were again submitted to ultrafiltration to yield a final protein concentration of about 700 μM. The partial reduction of the enzyme was achieved according to Ref. [33], using a solution of 100 mM $Na_2S_2O_4$ in 250 mM NaCl, 20 mM $Na_2P_2O_7$ pH (8.0). Reduction of the heme groups was monitored in the wavelength range of 500–600 nm using an SLM AMINCO DW-2000 spectrophotometer equipped with cuvettes of 2 mm path length ("Uvette", Eppendorf). The final reduction state was reached when both the absorbance at 562 nm and the absorbance at 554 nm showed nearly equal intensities. The sample was then immediately transferred to an EPR tube and frozen in liquid nitrogen.

The concentration of the samples was estimated by measuring the redox-difference spectrum of cytochrome $b$ absorbance between a fully reduced state with excess dithionite and a fully oxidized state with ferricyanide. The absorbance

coefficient for wavelength pair 562–575 nm (cytochrome $b$) was taken to be 25600 1 mol$^{-1}$ cm$^{-1}$.

## 2.2 EPR Spectroscopy

X-band cw-EPR spectra were recorded on a Bruker E-500 spectrometer with a standard rectangular Bruker EPR cavity (ER4102T), Q-band EPR spectra on a Bruker E-500 spectrometer with a standard Bruker resonator (ER 5106QT-W1). Both instruments were equipped with Oxford helium cryostats (ESR900 and CF935, respectively). The measured $g$ values were corrected for an offset against a known $g$ standard [1,1-diphenyl-2-picrylhydrazyl, $g = 2.00351 \pm 0.00002$].

X-band pulsed EPR measurements were performed on a Bruker E-680 spectrometer using a Bruker MD5-W1 EPR probe head equipped with Oxford helium (CF 935) cryostat. The microwave pulses were amplified using a 1 kW traveling-wave tube (Applied Systems Engineering, USA). The field-swept spectrum was obtained by integrating the two-pulse echo signal as a function of the magnetic field after a two-pulse sequence. The inversion-recovery field-swept spectra were obtained as described in Ref. [28] by integrating the area of the echo after detection of the three-pulse sequence ($\pi - T_F - \pi/2 - t - \pi$). Three-pulse ESEEM and ESEEM–REFINE experiments were performed as described in Refs. [28, 34].

## 3 Results and Discussion

Figure 2a shows the X-band cw-EPR spectra of the reduced cytochrome $bc_1$ complex from *S. cerevisiae* at 9 K. A broad signal from the reduced Rieske center is clearly visible, as well as an intense narrow signal situated at $g \sim 2.0042$ typical of a semiquinone [35]. The concentration of ubisemiquinone is determined to be about 60% relative to that of the reduced Rieske EPR signal, which is to be expected. The dashed spectrum in Fig. 2a is from the $bc_1$ complex reduced in the presence of the $Q_i$ site inhibitor antimycin [36]. Again at 9 K, a broad signal from the reduced Rieske center is clearly visible but now no narrow signal is observed clearly, indicating that the narrow signal observed in Fig. 1a results from a semiquinone in the $Q_i$ site.

Figure 2b shows the field-swept pulsed X-band EPR spectra of the reduced $bc_1$ complex from *S. cerevisiae*. This spectrum is recorded by integrating the two-pulse echo signal as a function of the magnetic field after a two-pulse sequence. Again a broad signal from the reduced Rieske center and an intense narrow signal are observed at 9 K. If this spectrum is recorded at higher temperatures, e.g., 80 K (dotted line), the narrow signal is present while the broad signal has disappeared.

At 80 K, we are able to resolve the $g$ anisotropy of this radical signal by performing EPR at higher microwave frequencies and magnetic fields (Fig. 2c). At Q-band (34 GHz), it has been shown that the $g$ tensor anisotropy of semiquinone radical anions can be partially resolved, e.g., for the $Q_H^{\bullet-}$ semiquinone radical anion in the *E. coli* terminal oxidase [34]. Simulation of this spectrum allows a direct determination of the $g$ tensor. These simulations have been carried out using an
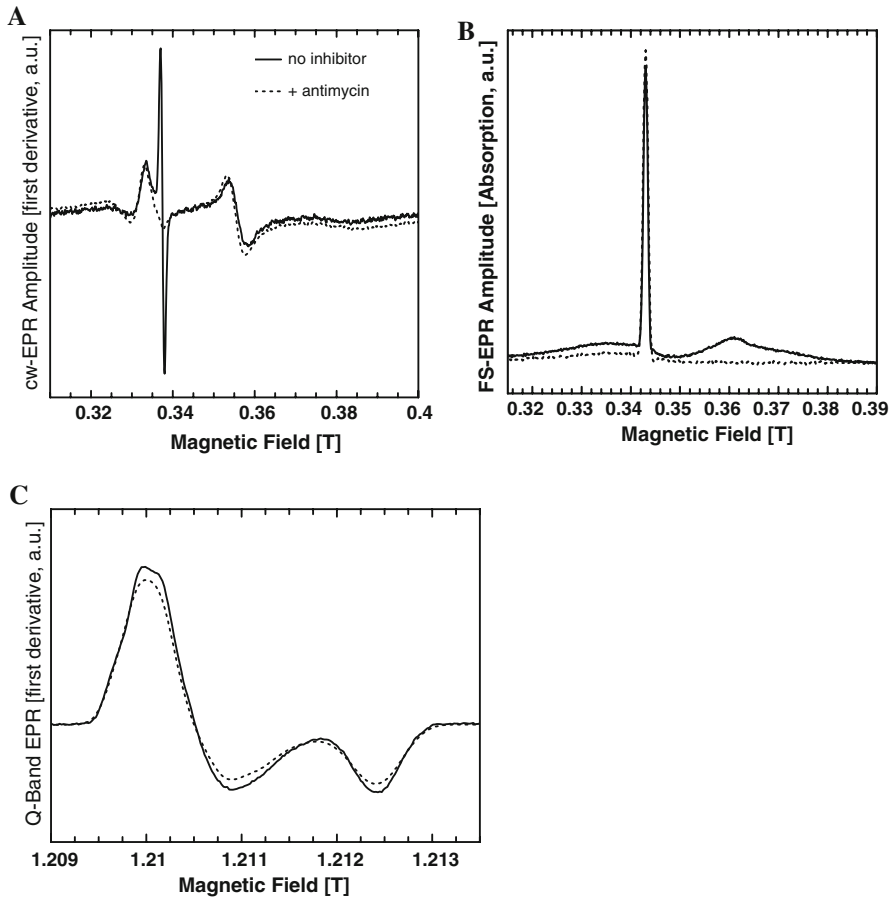
Fig. 2 **a** X-band cw-EPR spectra of the reduced $bc_1$-complex from yeast (*solid line*) and in the presence of antimycin A (*dashed line*). Experimental conditions: microwave power, 0.1 mW; field modulation frequency, 100 kHz; field modulation depth, 0.5 G; temperature, 20 K. **b** X-band field-swept pulsed EPR spectra of the reduced $bc_1$-complex from yeast. Experimental conditions: microwave frequency, 9.745446 GHz; $\pi/2$ pulse length, 8 ns; $\tau = 120$ ns; shot repetition rate, 1 ms; temperature, 20 K (*solid trace*) and 80 K (*broken trace*). **c** Q-band cw-EPR spectrum (*solid trace*) and simulation (*broken trace*) of the reduced $bc_1$-complex from yeast. Experimental conditions: microwave power, 2 mW; field modulation frequency, 10 kHz; field modulation depth, 1 G; temperature, 80 K

anisotropic line width parameter, characterized by a Gaussian line shape to account for hyperfine interactions from the methyl protons at position 5 and other smaller couplings (hydrogen bonded-, $CH_2$- and methoxy-protons). The observed $g$ tensor line widths used for simulations are given in Table 1.

Using an inversion-recovery pulse sequence, time traces can be recorded at different magnetic field positions [29], which observe the recovery of the $M_z$ magnetization, that is inverted by the first $\pi$ pulse. This recovery of magnetization can be monitored using a simple Hahn-echo pulse sequence across a range of magnetic field values. If two species (e.g., $Q_i^{\bullet-}$ and the Rieske FeS center) have different $t_1$ relaxation times, then different recovery times are observed (Fig. 3a).

**Table 1** $g$-Values of the $Q_i^{\bullet-}$ ubisemiquinone radical anion as determined from spectral simulation of Q-band cw-EPR spectra and a comparison with values for other ubisemiquinone radical anions from the literature

| Species | $g_{xx}$ | $g_{yy}$ | $g_{zz}$ | 1/3 (Tr $g$) | Ref. |
|---|---|---|---|---|---|
| $Q_i^{\bullet-}/bc_1$ | 2.0062 (1) | 2.0053 (1) | 2.0022 (1) | 2.00457 (1) | This work |
| $Q_H^{\bullet-}$/quinol oxidase | 2.00593 | 2.00543 | 2.0022 | 2.00452 | [34] |
| $Q_A^{\bullet-}$/bacterial reaction center | 2.00649 | 2.00532 | 2.00210 | 2.00464 | [37] |
| $UQ_{10}^{\bullet-}$/isopropanol | 2.00627 | 2.00531 | 2.00213 | 2.00457 | [35] |
| $UQ_3^{\bullet-}$/DME/mTHF[a] | 2.0070 | 2.00537 | 2.00202 | 2.0048 | [38] |

[a] *DME* dimethoxyethane; *mTHF* methyltetrahydrofolate

In Fig. 3a the observed relaxation times have been used to calculate the individual time traces for the two species as well as the sum of these two traces. By inspection it is clear that there is a point in time, where the net magnetization crosses zero, which is different for each of the individual time traces (indicated by the arrows in Fig. 3a). If one performs a field-sweep EPR experiment (as in Fig. 2b) at such times, then only one of the two species is detectable, at a reduced intensity. These so-called filter times ($T_F$) can be experimentally determined or calculated [28, 30]. Alternatively a two-dimensional experiment can be performed (Fig. 3b), where the field-swept EPR spectrum is measured as a function of this filter time ($T_F$). From this data set one can extract specific traces (Fig. 3c, d) to demonstrate that it is possible to suppress the contribution from the narrow radical species (Fig. 3d) and also, despite a significant degree of $t_1$ anisotropy, suppress the contribution from the broad Rieske signal at the field position corresponding to the narrow $Q_i$ radical signal (Fig. 3c).

In Fig. 3c, EPR spectra recorded at four different filter times are shown. At a very short filter time (lowermost trace in Fig. 3b), the responses from both the semiquinone and the Rieske center are inverted. Under the experimental conditions here (see legend to Fig. 3), we are able to invert about 15% of the semiquinone signal. At a slightly later time (in this case at 10 K, 870 µs), while the response from the semiquinone is still inverted, the response of the Rieske center is zero (at the magnetic field position corresponding to the resonance position of the semiquinone). Here a pure spectrum from $Q_i^{\bullet-}$ (yield $\sim$ 10%) can be obtained (middle trace in Fig. 3c). At a later time (8.7 ms, second uppermost trace in Fig. 3c), the response from the semiquinone is zero, and a spectrum from the Rieske center can be observed. At much later times, both signals can be observed (Fig. 3c, uppermost trace) again.

The ratio of relative amounts of species as well as their respective relaxation times determine how efficient this type of experiment can be. So far this technique has been applied to resolve overlapping organic radicals and spin labels as well as iron–sulphur centers (see Refs. [28, 30]). In the study presented here we apply this technique to refine the individual EPR spectra from a narrow organic radical and an iron–sulphur center.

ESEEM spectroscopy is a powerful tool to study the binding of semiquinones within their binding pockets in proteins [14] by observing the interaction with
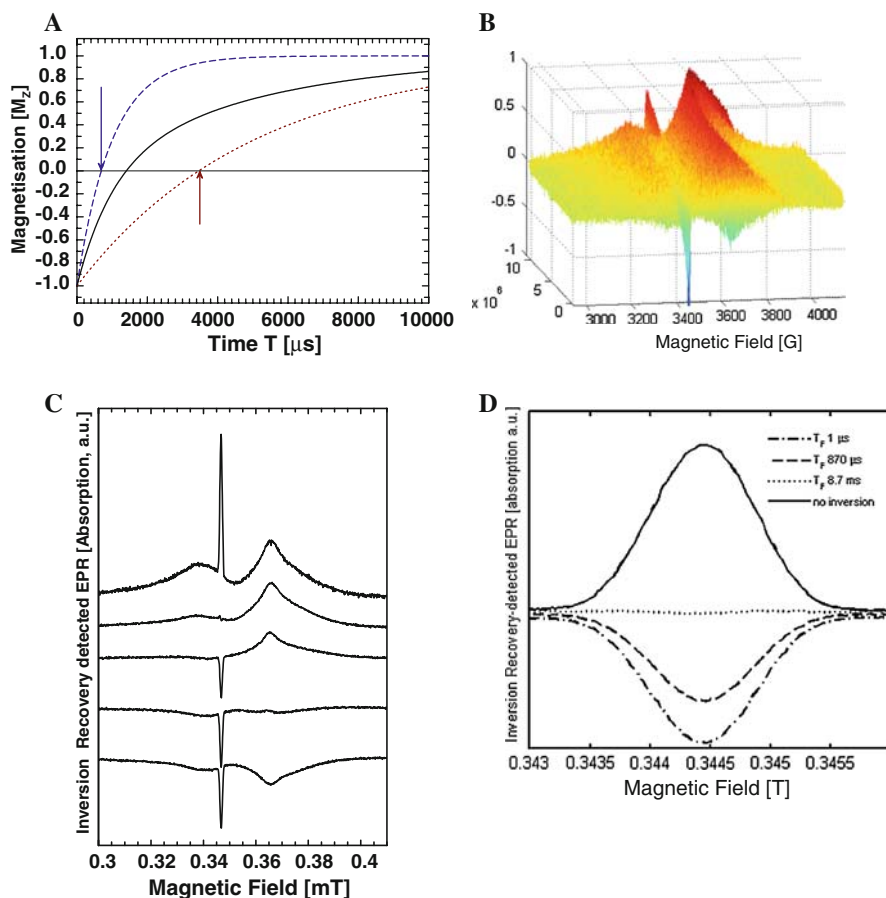
**Fig. 3 a** Plot of the time traces observed using the relaxation times of the individual species (*dashed and dotted traces*) and their sum (*solid trace*). Two times, indicated by the *arrows*, are when the recovery of individual $M_z$ magnetizations traverses zero. These times are used to filter the contributions of the individual species in the field-swept EPR spectra. **b** Two-dimensional plot of field-swept spectra versus the filter time $T_F$. **c** Selected spectra from **b** and **d** selected filter times ($T_F$) to measure a narrow field range around the semiquinone species. Experimental conditions for **b**, **c** and **d**: microwave frequency, 9.67944 GHz; $\pi/2$ pulse length, 8 ns; inversion pulse, 16 ns; $\tau = 120$ ns; shot repetition rate, 300 ms; temperature, 10 K

magnetic nuclei (typically $^{14}$N). Figure 4a shows the ESEEM time domain spectra of the reduced $bc_1$ complex recorded at the field position corresponding to semiquinone at 80 K (upper trace) and 9 K (lower trace). There are clear differences, which are more apparent when the data are Fourier transformed (Fig. 4b). The solid spectrum (9 K) contains intensity in the frequency ranges associated with both $^1$H (15 MHz) and $^{14}$N nuclei (0–8 MHz), while the dashed spectrum (80 K) only contains frequencies associated with $^1$H's. From Fig. 2b it is clear that at 80 K only the semiquinone species is contributing to the EPR spectrum, and thus the ESEEM spectra of this species contain no interactions with $^{14}$N nuclei, as predicted from the geometry of the binding from the X-ray structural model
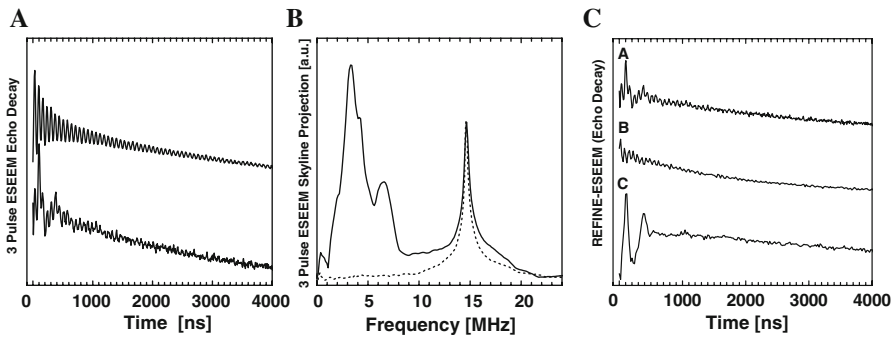
**Fig. 4** **a** Selected three-pulse ESEEM time traces recorded at a field position corresponding to the maximum signal intensity of the semiquinone species at 80 K (*upper*) and 9 K (*lower*). **b** Skyline representation of the Fourier transformation of a two-dimensional three-pulse ESEEM data set. $\tau$ was varied from 124 to 220 ns in steps of 12 ns. **c** REFINE–ESEEM time traces using no filter time (*a*), a filter time of 870 μs (*b*) and a filter time of 8.7 ms (*c*). Experimental conditions: microwave frequency, 9.67944 GHz; $\pi/2$ pulse length, 8 ns; inversion pulse, 16 ns; initial $\tau = 140$ ns; repetition rate, 300 ms; temperature, 9 K

(Fig. 1b). Recent similar experiments performed on the bacterial $bc_1$ complex from *Rb. sphaeroides* (where no high-resolution structure of $Q_i$ in the $Q_i$ binding pocket is available), however, propose a direct binding to histidine through observation of $^{14}N$ echo modulation at low temperatures [23, 24], although similar experiments on the related purple bacteria *Rhodobacter capsulatus* $bc_1$ do not show any $^{14}N$ modulations [F. MacMillan (University of East Anglia, Norwich, UK) and J. Cooley (University of Missouri, Columbia, USA), unpublished data].

In the case of the yeast $bc_1$ complex, $^{14}N$ echo modulation is also observed at 9 K, but we assign this to interactions associated with the Rieske iron–sulphur cluster. In order to resolve this discrepancy we have performed ESEEM spectroscopy in combination with the REFINE technique to selectively study both the semiquinone species and the Rieske iron–sulphur center at 9 K. From Fig. 3 it is clear that the relaxation behaviour of the Rieske center is clearly field-dependent (anisotropic). However, the ultimate aim is to use this filter together with the hyperfine experiment, which is performed at a static magnetic field. Therefore, it is only important to determine the filter time of the species one wishes to suppress at this static magnetic field.

Figure 4c contains three ESEEM time traces, the uppermost (trace *a*) is recorded without a REFINE inversion pulse and both fast and slow oscillation frequencies are observed from the $^1H$ and $^{14}N$ nuclei. When the REFINE–ESEEM experiment is performed using an 870 μs filter time (trace *b*), which corresponds to suppression of the Rieske center, we observe a clear suppression of the contribution from $^{14}N$ nuclei, whereas when the experiment is performed at 8.7 ms, the contribution from $^{14}N$ nuclei dominates. This clearly confirms the observation that the $Q_i^{\bullet-}$ species in the yeast $bc_1$ complex does not interact directly with a $^{14}N$ nuclei, which is in good agreement with the X-ray crystallographic model.

Density functional theory calculations performed using the coordinates from the yeast structure also confirm that (a) any observed interactions would be too weak to

be detected using EPR, and (b) energy minimization of the published structures, where a direct coordination of the quinone species with a $^{14}N$ nucleus results in a rearrangement of the structure such that the $^{14}N$ is again too far away from the semiquinone species to permit detection of the interaction using ESEEM spectroscopy [F. MacMillan (University of East Anglia, Norwich, UK), J. Fritscher (University of Frankfurt, Frankfurt, Germany) and C. Hunte (University of Leeds, Leeds, UK), unpublished results].

## 4 Conclusions

This is the first EPR/ESEEM report of a ubisemiquinone (USQ) in the $Q_i$ site of the yeast (*S. cerevisiae*) cytochrome $bc_1$ complex. Clear evidence that it is specifically bound to the protein is provided by the sensitivity to the inhibitor antimycin, and the observed *g* tensor is very typical of other bound semiquinone anion radicals, suggesting a tight binding through hydrogen bonds to the protein.

While it is generally accepted that the USQ anion radical is a stable intermediate in Q reduction at the $Q_i$ site, details of the USQ interaction with haem $b_H$ and possible ligands are still unresolved and $H^+$ pathways are debated. Three X-ray structures provide differing information, as they show different substrate binding patterns. The observed differences in the bovine, yeast and purple bacterium structures may be species related and/or due to different redox states of the structures. Using REFINE we have shown that it is now possible to study the semiquinone species individually in the $bc_1$-complex, using hyperfine spectroscopy to resolve the important question of its binding to the protein.

## References

1. C. Hunte, S. Solmaz, H. Palsdottir, T. Wenz, Results. Probl. Cell Differ. **45**, 253–278 (2008)
2. A.R. Crofts, Annu. Rev. Physiol. **66**, 689–733 (2004)
3. P. Mitchell, J. Theor. Biol. **62**, 327–367 (1976)
4. C. Hunte, J. Koepke, C. Lange, T. Rossmanith, H. Michel, Struct. Fold. Des. **8**, 669–684 (2000)
5. C. Hunte, FEBS Lett. **504**, 126–132 (2001)
6. C. Lange, J.H. Nett, B.L. Trumpower, C. Hunte, EMBO J. **20**, 6591–6600 (2001)
7. L.S. Huang, D. Cobessi, E.Y. Tung, E.A. Berry, J. Mol. Biol. **351**, 573–597 (2005)
8. X. Gao, X. Wen, L. Esser, B. Quinn, L. Yu, C.A. Yu, D. Xia, Biochemistry **42**, 9067–9080 (2003)
9. H. Zhang, A. Osyczka, P.L. Dutton, C.C. Moser, Biochim. Biophys. Acta **1767**, 883–887 (2007)
10. J.L. Cape, M.K. Bowman, D.M. Kramer, Proc. Natl. Acad. Sci. USA **104**, 7887–7892 (2007)

11. S. Junemann, P. Heathcote, P.R. Rich, J. Biol. Chem. **273**, 21603–21607 (1998)
12. T. Ohnishi, B.L. Trumpower, J. Biol. Chem. **255**, 3278–3284 (1980)
13. J.C. Salerno, M. Osgood, Y.J. Liu, H. Taylor, C.P. Scholes, Biochemistry **29**, 6987–6993 (1990)
14. T. Prisner, M. Rohrer, F. MacMillan, Annu. Rev. Phys. Chem. **52**, 279–313 (2001)
15. F. Lendzian, J. Rautter, H. Käß, A. Gardiner, W. Lubitz, Ber. Bunsenges., Phys. Chem. Chem. Phys. **100**, 2036–2040 (1996)
16. A.P. Spoyalov, R.J. Hulsebosch, S. Shochat, P. Gast, A.J. Hoff, Chem. Phys. Lett. **263**, 715–720 (1996)
17. Y. Deligiannakis, A. Boussac, A.W. Rutherford, Biochemistry **34**, 16030–16038 (1995)
18. J. Hanley, Y. Deligiannakis, F. MacMillan, H. Bottin, A.W. Rutherford, Biochemistry **36**, 11543–11549 (1997)
19. C. Jegerschöld, F. MacMillan, W. Lubitz, A.W. Rutherford, Biochemistry **38**, 12439–12445 (1999)
20. S. Grimaldi, F. MacMillan, T. Ostermann, B. Ludwig, H. Michel, T. Prisner, Biochemistry **40**, 1037–1043 (2001)
21. M.T. Lin, R.I. Samoilova, R.B. Gennis, S.A. Dikanov, J. Am. Chem. Soc. **130**, 15768–15769 (2008)
22. J. Abramson, S. Riistama, G. Larsson, A. Jasaitis, M. Svensson-Ek, L. Laakkonen, A. Puustinen, S. Iwata, M. Wikstrom, Nat. Struct. Biol. **7**, 910–917 (2000)
23. D.R. Kolling, R.I. Samoilova, J.T. Holland, E.A. Berry, S.A. Dikanov, A.R. Crofts, J. Biol. Chem. **278**, 39747–39754 (2003)
24. S.A. Dikanov, J.T. Holland, B. Endeward, D.R. Kolling, R.I. Samoilova, T.F. Prisner, A.R. Crofts, J. Biol. Chem. **282**, 25831–25841 (2007)
25. T.F. Prisner, in *Advances in Magnetic and Optical Resonance*, vol. 20, ed. by W. Warren (Academic Press, New York, 1997), p. 245
26. S. Stoll, G. Jeschke, M. Willer, A. Schweiger, J. Magn. Reson. **130**, 86–96 (1998)
27. C.C. Lawrence, M. Bennati, H.V. Obias, G. Bar, R.G. Griffin, J. Stubbe, Proc. Natl. Acad. Sci. USA **96**, 8979–8984 (1999)
28. T. Maly, F. MacMillan, K. Zwicker, N. Kashani-Poor, U. Brandt, T.F. Prisner, Biochemistry **43**, 3969–3978 (2004)
29. A. Schweiger, G. Jeschke, *Principles of Pulse Electron Paramagnetic Resonance* (Oxford University Press, Oxford, 2001)
30. T. Maly, T.F. Prisner, J. Magn. Reson. **170**, 88–96 (2004)
31. H. Palsdottir, C.G. Lojero, B.L. Trumpower, C. Hunte, J. Biol. Chem. **278**, 31303–31311 (2003)
32. H. Palsdottir, C. Hunte, in *Membrane Protein Purification and Crystallisation: A Practical Guide*, 2nd edn., ed. by C. Hunte, G. von Jagow, H. Schägger (Academic Press, New York, 2003), pp. 191–203
33. F.F. de la Rosa, G. Palmer, FEBS Lett. **163**, 140–143 (1983)
34. S. Grimaldi, T. Ostermann, N. Weiden, T. Mogi, H. Miyoshi, B. Ludwig, H. Michel, T.F. Prisner, F. MacMillan, Biochemistry **42**, 5632–5639 (2003)
35. O. Burghaus, M. Plato, M. Rohrer, K. Mobius, F. MacMillan, W. Lubitz, J. Phys. Chem. **97**, 7639–7647 (1993)
36. E.C. Slater, Biochim. Biophys. Acta **301**, 129–154 (1973)
37. J.S. van den Brink, A.P. Spoyalov, P. Gast, W.B. van Liemt, J. Raap, J. Lugtenburg, A.J. Hoff, FEBS Lett. **353**, 273–276 (1994)
38. O. Nimz, F. Lendzian, C. Boullais, W. Lubitz, Appl. Magn. Reson. **14**, 255–274 (1998)